Journal of Hydrology: Regional Studies 54 (2024) 101865

Contents lists available at ScienceDirect

Journal of Hydrology: Regional Studies

journal homepage: www.elsevier.com/locate/ejrh

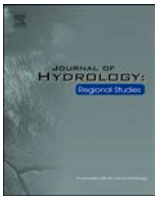

A multi-method approach for assessing groundwater vulnerability of shallow aquifers in the Marchfeld region (Austria)

Francesco Fusco [a,b], Vincenzo Allocca [b,c], Marialaura Bancheri [c,d,*], Angelo Basile [c,d], Domenico Calcaterra [b,c], Antonio Coppola [e,f], Martin Neuwirth [g], Àngela Puig-Sirera [h], Fabio Terribile [c,i], Pantaleone De Vita [b,c]

[a] Department of Civil and Environmental Engineering, Politecnico di Milano, Piazza Leonardo da Vinci, 32, Milan 20133, Italy
[b] Department of Earth, Environment and Resources Sciences, University of Naples Federico II, Complesso Universitario di Monte Sant'Angelo, Via Cinthia, 21, Naples 80126, Italy
[c] CRISP Research Center. University of Naples Federico II, Via Università, 100, Portici, NA 80055, Italy
[d] Institute for Mediterranean Agricultural and Forestry Systems (ISAFOM), National Research Council (CNR), Piazzale E. Fermi, 1, Portici, NA 80055, Italy
[e] School of Agricultural, Forestry, Food and Environmental Sciences (SAFE), Hydraulics Division, University of Basilicata Macchia Romana Campus, Viale dell'Ateneo Lucano, 10, Potenza 85100, Italy
[f] Department of Chemical and Geological Sciences, University of Cagliari, Via Università, 40, Cagliari 09124, Italy
[g] Umweltbundesamt – Environment Agency Austria (EAA), Spittelauer Lände 5, Wien 1090, Austria
[h] University of Pisa, Department of Agriculture, Food and Environment (DAFE), Via del Borghetto, 80, Pisa 56124, Italy
[i] Department of Agriculture, University of Napoli Federico II, Via Università, 100, Portici, NA 80055, Italy

ARTICLE INFO

Keywords:
Groundwater vulnerability
PCSM methods
Numerical models
SINTACS
TFM-ext
FLOWS

ABSTRACT

Study region: Marchfeld region (Austria)
Study focus: A multi-method and multi-scale assessment of the intrinsic groundwater vulnerability to generic pollutants was carried out. At the regional scale, a parametric method, to assess the intrinsic groundwater vulnerability, and a transfer function model, to assess the travel time of a generic and non-reactive pollutant through the unsaturated zone, were applied. At the site-specific scale, the travel time of the peak concentration was evaluated by using a physically-based hydrological model. The comparison of results of different approaches allowed mutual validation and advanced the knowledge about the assessment of groundwater vulnerability.
New hydrogeological insights for the region: To assess the groundwater vulnerability, a detailed hydrogeological map of the study area was reconstructed. A large variability of hydrogeological, morphological and anthropic conditions was recognized. Alluvial aquifers formed by high-permeability deposits hosting shallow groundwater circulation are characterized by the highest groundwater vulnerability. Contrarily, lower groundwater vulnerability was recognized for aquifers formed by low-permeability deposits, favoring a reduction of infiltration processes and a major attenuation of pollutants' potential effects. The presented multi-method approach revealed how comparing the results of a DRASTIC-like method and two process-based models can deliver hints regarding their suitability, different spatial densities and quality of required inputs, and effectiveness. Finally, the potential strong impact of some agricultural practices was confirmed.

* Corresponding author at: Institute for Mediterranean Agricultural and Forestry Systems (ISAFOM), National Research Council (CNR), Piazzale E. Fermi, 1, Portici NA, 80055, Italy.
E-mail address: marialaura.bancheri@cnr.it (M. Bancheri).

https://doi.org/10.1016/j.ejrh.2024.101865
Received 22 April 2024; Received in revised form 7 June 2024; Accepted 8 June 2024

1. Introduction

Industrial and agricultural activities are the main causes of groundwater pollution and the decay of the hydro-chemical quality of groundwater (Zektser and Everett, 2000), which represents the most important source of drinking water for many countries. Therefore, assessing groundwater vulnerability is a crucial aspect of proper land planning and management, as well as the implementation of effective groundwater protection strategies (e.g., GSD 15; Directive 2000/60/EC; Directive 91/676/EC; Directive 2009/128/EC).

Groundwater vulnerability is generally distinct in intrinsic, defined as "*the specific susceptibility of aquifer systems, (…) to ingest and diffuse fluid and/or hydro-vehiculated contaminants, whose impact on groundwater quality is dependent on space and time*" (Civita, 1994), and specific, related to a definite contaminant, considering the related specific hydraulic and geochemical processes of attenuation (National Research Council (NRC (NRC, (1993); Gogu and Dassargues, (2000)).

For such a scope, three fundamental categories of approaches to assess groundwater vulnerability are known (Civita, 2010): 1) Hydrogeological Complexes and Settings (HCS) methods, based on qualitative analysis of hydrogeological factors such as geological aspects of the saturated/unsaturated zone, main hydraulic properties of lithologies, depth of the water table, physical and chemical characteristics of soils and net recharge (Albinet and Margat, 1970); 2) Parametric System (PS) methods, divided into three sub-groups: Matrix Systems (MS) (Goossens and Van Damme, 1987), Rating Systems (RS), such as GOD method (Foster, 1987), and Point Count System Models (PCSM), such as DRASTIC (Aller et al., 1985) and SINTACS (Civita and De Maio, 2000) methods, are based on semi-quantitative assessment of factors controlling groundwater vulnerability (such as soil thickness and texture, water table depth and aquifer hydrogeological features (e.g., Cusano et al., 2019; Turc, 1954; Tufano et al., 2020; Cusano et al., 2023); and Numerical Models (NM), such as those estimating travel times (TT) of pollutants through the unsaturated zone (Brouyère et al., 2001; Neukum and Azzam, 2009; Nasta et al., 2021; Stewart and Loague, 2003; Fusco et al., 2020; Bancheri et al., 2021), based on quantitative assessment of groundwater vulnerability through modeling of the physical, chemical, and biological processes controlling the transport of a pollutant. The application of parametric and numerical methods is related respectively to regional and site-specific scales because requiring data of different quality and spatial density. The greater level of complexity of the second one, depending on the quality of data required to solve equations governing flow and transport processes, in unsaturated and/or saturated porous media, limits their applicability to the site-specific scale instead of regional one. Consequently, a comparison among the results of both classes of methods can be conceived as particularly useful to explore the mutual limitations, especially in terms of scales of application, and thus to select the most effective one depending on available data.

Several studies are based on the comparative assessment of groundwater vulnerability performed through only parametric methods (Draoui et al., 2008; Kirlas et al., 2022). Instead, the comparison of such methods with numerical ones appears rare and not considered

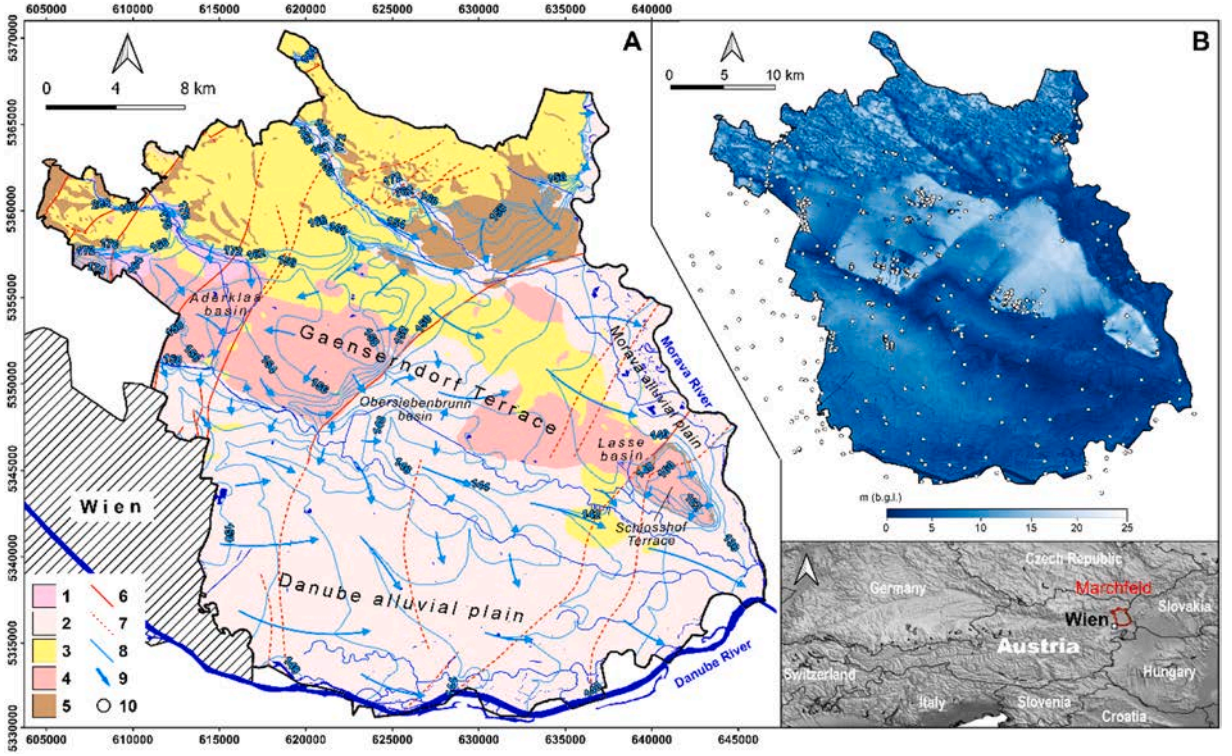

Fig. 1. - Hydrogeological (A) and groundwater table depth (B) maps reconstructed for Marchfeld Region: 1) Recent fine-graded alluvial Complex (RFAC); 2) Recent Alluvial Complex (RAC); 3) Löess Complex (LC); 4) Ancient Alluvial Complex (AAC); 5) Basin Argillaceous Complex (BAC); 6) Faults; 7) Presumed faults; 8) Main hydrographic network; 9) Groundwater flow direction. (WGS84, UTM33N).

carefully (Abbasi et al., 2013), depending on different structures of methods and types of results that are not directly comparable.

In such a framework, the benefit of the procedure proposed is to offer an insight into the assessment of groundwater vulnerability to pollution as well as to verify the reliability of qualitative methods in comparison to the numerical ones (Machiwal et al., 2018).

The goal of this work was the multi-scale and multi-method estimation and mapping of intrinsic groundwater vulnerability of the representative shallow alluvial aquifer system characterizing the Marchfeld region (northern Austria; Fig. 1) by coupling parametric and numerical approaches and comparing respective results. Due to its large extension, covering about 1000 km^2, and the dominant agricultural land use, the Marchfeld region represents a primary source of agricultural products for the Austrian/European markets. This area was considered representative because severely impacted by intensive agriculture activities causing groundwater pollution by nitrates, with concentrations constantly above the allowable threshold level (Kirchner and Schmid, 2012). Thus, to obtain a comprehensive assessment of the groundwater vulnerability, from regional to site-specific scales, the parametric method SINTACS (Civita and De Maio, 2000) and two numerical ones, TFM-ext model (Bancheri et al., 2021) and the RE-ADE-based agro-hydrological model FLOWS (Coppola et al., 2014; 2019), were considered. For such a scope, consistent bibliographic research and consultation of ministerial and municipal archives allowed the reconstruction of a detailed geodatabase, structured in a GIS environment, containing fundamental informative layers such as geological, hydrogeological, pedological and climate features. Finally, the results of parametric and numerical methods were mutually compared revealing hints regarding the limits and suitability of the different classes of methods. In the wake of the increasing development and usage of Decision Support Systems (DSS) (Yalew et al., 2016; Lindblom et al., 2017; Zaza et al., 2018; Marano et al., 2019; Manna et al., 2020; Nicholson et al., 2020; Terribile et al., 2023), the obtained results represent potential powerful tools for accurate assessment of potential groundwater degradation in areas affected by intensive agricultural activities. Specifically, results are expected to be considered by a wide range of stakeholders such as land managers (i.e., public authorities), to properly evaluate more informed decisions regarding the areas in which the pollution from agricultural activities should be primarily reduced.

2. Data and methods

2.1. Geological and hydrogeological setting

The Marchfeld region is in northern Austria and northeast of Vienna (Fig. 1). The region is a Temperate Continental Climate / Humid Continental Climate (Dfb) according to the Köppen classification (Geiger, 1954), with a mean annual precipitation of about 500–550 mm, an average temperature between 9 and 10 °C and a mean annual reference potential evapotranspiration of about 800 mm. Geologically, the study area roughly coincides with the Quaternary alluvial plain in the central part of the Vienna Basin, which is a SSW-NNE oriented Neogene pull-apart basin of about 200 km length and 55 km width, extended from the eastern Austrian Alps to the western Carpathians in the Czech Republic. An intensive tectonic activity involved the area (Decker et al., 2005) causing a sinking process forming depressions filled by Miocene clastic sequence (shales, sandstones, conglomerates) and subordinate shallow-water limestones up to 5.5 km thick (Holzel et al., 2008). Such deposits overlie with a marked angular unconformity in the pre-Miocene basement (Wessely, 1993). Finally, alluvial Pleistocene deposits, formed by up to 140 m of alternating fluvial sands and gravels intercalated by pedogenized horizons, overlay the Miocene series (Decker et al., 2005). A Quaternary tectonic activity formed a series of river terraces between the basin margin in the west and the *Morava River* floodplain in the east, among them the most prominent is the *Gaenserndorf Terrace*. Moreover, the subsidence process that occurred during the Quaternary determined the fragmentation of terraces and the formation of small depressions, such as the *Aderklaa*, *Obersiebenbrunn*, and *Lasse basins* (Weissl et al., 2017).

Accordingly, the Marchfeld region is characterized by a Quaternary aquifer system, constituted by alluvial and loess sediments overlying Miocene deposits (Wessely and Draxler, 2006), which represents one of the most important porous aquifers of Austria. Based on geological information, locally improved by stratigraphic logs derived from 596 boreholes (Table 1), a detailed hydrogeological map of the study area was reconstructed (Fig. 1 A). The sedimentary series were grouped into five hydrogeological complexes as follows (Table 2):

Table 1
Main characteristics of the hydrogeological complexes defined for the Marchfeld region in this study.

Hydrogeological complex	Lithologies	Age	Type	Characteristic
Recent Fine-graded Alluvial Complex (RFAC)	Alluvial deposits: clay, loam and locally sand, gravel	Pleistocene - Holocene	Porous	Local aquifer
Recent Alluvial Complex (RAC)	Alluvial-eluvial deposits (recent terrace orders of Danube River and its tributaries): sand, gravelly sand, gravel, loamy gravel; secondly loess deposits	Pleistocene - Holocene	Porous	Regional aquifer
Loess Complex (LC)	Aeolic deposits (Loess): fine sand, clayey loam	Pleistocene - Holocene	Porous	Local aquifer/ aquitard
Ancient Alluvial Complex (AAC)	Alluvial deposits (oldest terrace order of Danube River and its tributaries): cobbles, gravel, sand, loam; locally loess deposits	Pleistocene	Porous	Local aquifer
Basin Argillaceous Complex (BAC)	Basin marine deposits: mainly clay, marl and sand, locally gravel, sandstone and conglomerate; locally loess-covering deposits	Eocene - Miocene	Porous/ fractured	Aquitard

- *Recent Fine-graded Alluvial Complex* (RFAC), mainly characterized by alluvial fan deposits (Pleistocene-Holocene) with grain sizes varying from clays to sands (and to gravels, locally);
- *Recent Alluvial Complex* (RAC), characterized by stratified alluvial-eluvial deposits (Pleistocene-Holocene), locally covered by loess sediments, with grain sizes varying mainly from sand to gravels and locally clays, coinciding with Danube and Morava alluvial plains;
- *Ancient Alluvial Complex* (AAC), formed by the oldest terraced alluvial deposits of the *Gaenserndorf Terrace* (Pleistocene-Middle Pleistocene), locally covered by loess deposits, with grain sizes mainly varying from sand to cobbles;
- *Loess Complex* (LC), including the fine-graded loess deposits (Pleistocene-Holocene), ranging from clayey loams to fine sands;
- *Basin Argillaceous Complex* (BAC), mainly constituted by clays, marls and sands and subordinately by gravels, sandstones and conglomerates (Miocene), locally covered by loess.

According to typical range values of hydraulic conductivity known in the literature (Freeze et al., 1979; Darsow et al., 2009), mainly BAC and secondarily LC and RFAC represent the hydrogeological complexes with lower permeability (1×10^{-10}, 1×10^{-7} and 1×10^{-6} m s^{-1}, respectively) due to the occurrence of finer deposits; while RAC and AAC are characterized by the higher permeability (1×10^{-4} and 1×10^{-1} m s^{-1}, respectively), as resulting by the occurrence of coarse grain sizes.

Literature piezometric levels from 424 boreholes, 167 wells and water table contour maps (Table 2) were analysed allowing the reconstruction of the Ground Water Table Depth (GWTD) map of the shallowest aquifer (Fig. 1B). Generally, the RAC and RFAC are characterized by low values of GWTD (1.0 – 5.0 m down to 15.0 – 20.0 m) in areas coinciding with the Morava alluvial plain and the Danube one, specifically along the north-eastern sector bordering the *Graeserndorf Terrace* and the southern one. Furthermore, diffuse surfacing of groundwater, such as artificial or natural ponds and channels was observed. Due to morphological features shaping the central sector of the Marchfeld region, relatively higher GWTD values (down to 25.0 m) were observed for the AAC and LC in areas coinciding with the *Gaenserndorf Terrace* and the *Schlosshof Terrace*. Values ranging between 8.0 and 20.0 m of GWTD characterize the more elevated areas of the north-western and central sectors of these terraces. However, also limited areas with low values of GWTD (1.0 – 5.0 m) or groundwater surfacing occur coinciding with artificial morphological depressions, related to anthropogenic excavations (quarries). Finally, the northern sector corresponding to the hilly areas of Marchfeld (BAC and LC) is generally characterized by a GWTD range between 3 and 6 m with peaks of 15 m in limited areas.

Based on this hydro-stratigraphic setting characterizing the Marchfeld region, the circulation of the shallowest groundwater is generally north-western–south-western oriented (Fig. 1 A), with a very low piezometric gradient (0.6 ‰ up to 1 ‰), according to literature (Darsow et al., 2009).

Among the main observations, generalized divergences of groundwater flow characterize the sector of the *Gaenserndorf Terrace* bordering the northern hilly landscapes, with drainage direction oriented toward the *Morava Plain*, in the eastern sector, and *Danube Plain*, in the western one. A local increase of piezometric gradient as well as changes in flow direction occurs along the north-western border of the *Obersiebenbrunn basin* and toward the bordering alluvial plain resulting in the *Schlosshof Terrace*, where a radial groundwater flow exists. Such conditions can be related to the occurrence of tectonic features and stratigraphic settings.

2.2. The SINTACS method

The SINTACS parametric method (Civita and De Maio, 2000) was considered to assess groundwater vulnerability at the regional scale. This method derives from a modification of DRASTIC (Aller et al., 1987) method, which is based on different criteria for the attribution of scores to the same seven parameters, even if these are considered with a diverse acronym due to the Italian translation and changed order: S = depth to groundwater; I = Net recharge; N = Attenuation effect of unsaturated zone; T = Soil media; A = Aquifer media; C = Hydraulic conductivity of the aquifer; S = Topography. By the attribution of scores and weights (w_i) to each parameter, the calculation of the SINTACS index ($I_{SINTACS}$) is given by the Eq. (1):

Table 2
Source of geological, hydrogeological, pedological, climatic and land use data collected in this study.

Information	Bibliographic data	Ministerial or municipal archives
Geology	- GEOFAST cartography 1:50000 (geologie.ac.at/en/services/web-services) - Weissl et al., (2017) - Doppler et al., (2011)	- HADES archive (Bohrungsdatenbank der Niederösterreichischen Landesregierung)
Hydrogeology and piezometry	- Hydrogeological map of Austria 1:250000 (geologie.ac.at/en/services/web-services)- - Fank et al., (2008)	- HADES archive - eHYDA archive (https://ehyd.gv.at/#)
Pedology	- Soil type map 1:25000 (bfw.ac.at/rz/bfwcms.web?dok=1004043)	
Climatic		- Weather stations of Zwerndorf, Gross-Enzersdorf, Wolkersdorf, Bad Deutsch-Altenburg OE3
Land use	- CORINE Land Cover 2018 (land.copernicus.eu/pan-european/corine-land-cover)	
Geomorphology	- Digital Elevation Model (DEM) 10×10m (data.gv.at/katalog/dataset/d88a1246–9684–480b-a480-ff63286b35b7)	

$$I_{SINTACS} = S \times w_i + I \times w_i + N \times w_i + T \times w_i + A \times w_i + C \times w_i + S_l \times w_i \quad (1)$$

According to empirical criteria established for each parameter (Civita and De Maio, 2000), the scores are assigned ranging between 1 and 10 and indicating proportionally the relevance to groundwater vulnerability. The method establishes a fixed weight value for each parameter depending on five lines of weights chosen for different environmental conditions (normal impact, intense impact, karst, drainage from freshwater to groundwater bodies, fractured rocks). Therefore, the multiplying weights are attributed depending on both geological and hydrogeological settings as well as to land use of the study area, based on the CORINE land cover map (www.land.copernicus.eu/pan-european/corine-land-cover). Specifically, areas of normal impact with no critical conditions due to anthropic effect and land use were identified in forests, cultivated areas, etc.; areas of intense impact, with high anthropic effects and occurrence of potential pollutant sources, were recognized in urbanized areas, factories, intensive agricultural areas, etc.; the drainage areas were identified in areas where continuous or sporadic drainage processes from surficial or sub-surficial groundwater bodies occur; finally, karst and fractured rocks are not represented in the area.

2.2.1. Depth to water table (the S-parameter)

This parameter accounts for the travel length, and time, of pollutants from the ground down to the saturated zone, through the unsaturated one. Therefore, it is conceptually conceived as directly controlling the attenuation of the initial pollutant concentration. Due to the extension of the study area and the occurrence of areas with a complex hydrogeological setting, the assessment of GWTD (with 50-m resolution) was carried out by different data and approaches. For the alluvial areas, available piezometric data from boreholes and wells (Table 2), points of the natural surfacing of groundwater circulation (such as springs, rivers, ponds, etc.) and piezometric data from the bibliography (Fank et al., 2008) were considered. Instead, for northern areas coinciding with small aquifers and aquitards, constituted by loess deposits covering turbidite and basin series (flysch), a general lack of piezometric measurements led to assuming constant water table depth values, equal to 6.0 m and 3.5 m respectively, as commonly observed for such hydrogeological complex.

2.2.2. Net recharge or infiltration (the I-parameter)

This parameter represents the amount of precipitation recharging groundwater (Healy, 2010), therefore precipitation (P) minus the loss due to reference evapotranspiration (ETR) and runoff (R). It constitutes both the main vehicle for pollutants toward the saturated zone as well as a potential diluent that can diminish their concentrations. To estimate the mean annual groundwater recharge for the study area, data from four representative weather stations were considered (Table 2). Firstly, the cumulative annual precipitation (P) was estimated by considering daily records, from 1997 to 2016. Thus, the mean annual value was obtained as the average of the four 10-year rainfall time series. To estimate the yearly real evapotranspiration amount, Turc's (1954) empirical formula was adopted. Subsequently, the mean annual effective annual precipitation (P - ETR) was calculated and final net recharge for each hydrogeological complex was estimated empirically by multiplying it by the Groundwater Recharge Coefficient (GRC) derived by previous studies (Civita and De Maio, 2000; De Vita et al., 2018). Therefore, considering hydrogeological features of the hydrogeological complexes, the following values of GRC were assigned: 0.3 for RFAC and LC; 0.4 for RAC; 0.5 for AAC; and, finally, 0.1 for BAC.

2.2.3. Impact of vadose zone (the N-parameter)

This parameter accounts for the attenuation of pollutants during the transport through the unsaturated zone (UNSZ). It is meant to be dependent on the lithology, and, subsequently, hydraulic conductivity, of the vadose zone. Therefore, it was estimated by the hydrogeological map reconstructed for the Marchfeld region considering the lithology of the UNSZ of aquifers. To assess this parameter, the possible occurrence of local complex and heterogeneous hydrogeological settings, such as those characterized by paleochannels, was assumed as negligible according to the regional scale of analysis as well as to the spatial distribution of geological and hydrogeological input data

2.2.4. Soil media (the T-parameter)

This parameter depends on the grain size and controls the reactive processes occurring in the soil leading to the reduction of pollutant concentration. It was estimated by the soil map, 1:10,000 scale, available for the study area (Table 2). *Chernozem* and *fluvisol* are the main soils recognized, showing A and B (Legrain et al., 2018) silt-rich horizons and sandy deep soil horizons, the latter followed by fluvial gravel from the former riverbed of the Danube.

2.2.5. Hydrogeological characteristic of the Aquifer (the A-parameter)

This parameter, corresponding to the aquifer type of, describes all processes occurring in the saturated zone (dispersion, dilution, adsorption and chemical transformation). It is intended to be dependent on saturated hydraulic conductivity and mechanisms of saturated flow (e.g., porous, fractures) because expressing the capability and the time to transport of a pollutant through the saturated zone. This parameter was obtained by the hydrogeological map. As for the N-parameter, local heterogeneities were disregarded due to the regional scale of analysis as well as to the spatial distribution of geological and hydrogeological input data.

2.2.6. Aquifer's hydraulic Conductivity (the C-parameter)

This parameter indicates the capacity of the saturated zone to convey groundwater (and pollutants) through a unitary draining section and under an ordinary piezometric gradient. Therefore, it was conceived as indicating proportionally the susceptibility to pollution. This parameter was estimated by attributing to the aquifer type the mean value from ranges known in the literature (Freeze

et al., 1979; Civita and De Maio, 2000). As for the N-parameter, local heterogeneities were disregarded due to the regional scale of analysis as well as to the spatial distribution of geological and hydrogeological input data.

2.2.7. Slope (the S_I-parameter)

This parameter expressing the slope gradient, and accounting inversely for the predisposition to infiltration, and groundwater recharge was estimated by the DEM available for the area (Table 2).

2.3. The TFM-ext model

To assess groundwater vulnerability at the regional scale, also the Extended Transfer Function Model (TFM-ext) (Bancheri et al., 2021) was used. It represents an extension of the transfer function approach (Jury et al., 1990), and describes the leaching behaviour in a soil profile and along the vadose zone, till the groundwater table, through the Travel Time (TT) probability density functions (TT pdfs). The output solute concentration C_z (z,t) (i.e., the breakthrough curve), at a given time (t) and depth of interest (z), is computed as the convolution of the TT pdfs, f_f (z,t-t′) with the solute input concentration to the system, C_0 (0,t), according to the Eq. (2) (Jury and Roth, 1990):

$$C_z(z,t) = \int_0^T C_0(0,t') \quad f_f(z, \quad t-t')dt' \tag{2}$$

where t′ is a dummy variable and t-t′ is the TT.

Assuming a gravity-driven water flow and disregarding the convective mixing of tracer flowing at different velocities, in this approach the TT pdfs are calculated as functions of the unsaturated hydraulic conductivity K(θ), according to the Scotter and Ross (1994) Eq. (3):

$$f_f(z,t-t') = -\frac{1}{q}\frac{dK(\theta)}{dt} \tag{3}$$

where q [L T^{-1}] is the steady-state flow rate, which, in this study, is the constant mean daily net precipitation at the surface of the considered soil profile.

Under a lack of information regarding the unsaturated hydraulic conductivity function (e.g., in the vadose zone), the model assumes that the TT can be described by a log-normal distribution, according to the Generalized Transfer Function (Zhang, 2000). The

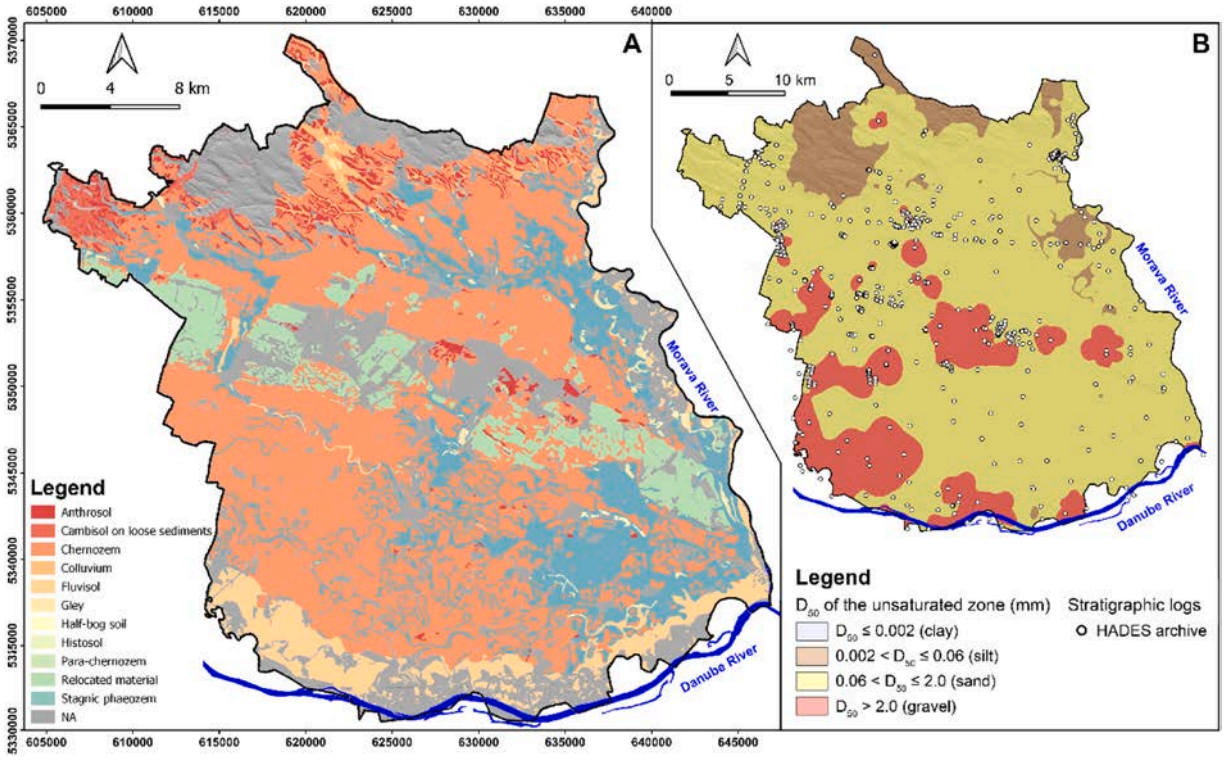

Fig. 2. - Map of soil types (A) and representative grainsize of the unsaturated zone (B) (UNSZ) reconstructed for Marchfeld Region. (WGS84, UTM33N).

detailed descriptions of the input data of the TFM-ext are reported in the following.

2.3.1. Net precipitation

This parameter coincides with the constant mean daily net precipitation computed from the difference between the amount of annual rainfall (Table 2) and the actual evapotranspiration. In this case, the latter was calculated from the potential evapotranspiration through the FAO model (Allen et al., 1998), considering both crop and water stress coefficients of the wheat. For such a scope, the period from January 2013 to December 2016 was considered.

2.3.2. Soil and UNSZ characterization

The soil units characterizing the study area (Fig. 2 A) were considered to define both soil and UNSZ characteristics. The dominant soil types are *Chernozem* and *Fluvisol*, comprising humus-rich surficial horizons and sandy deep ones. Instead, mainly fluvial gravels characterize the former riverbed of the Danube and Morava rivers. For each soil type, besides the depth of each soil horizon, the soil hydraulic parameters of the van Genuchten-Mualem equation (Van Genuchten, 1980) were estimated through the application of the HYPRES pedotransfer function (Wösten et al., 2001), starting from the pedological characterization (textures, bulk densities and organic matter content). To characterize the UNSZ, the representative grain size of soils forming the UNSZ for the entire territory of Marchfeld was estimated, based on the GWTDs map and stratigraphic data obtained by boreholes. Specifically, representative (qualitative) grain size curves were defined for each soil layer. Where percentages of grain size classes were not available from the stratigraphic logs, they were derived by soil description according to the AGI (1977) classification. Consequently, a representative value of the grain size diameter of the UNSZ was appraised for each borehole by the application of the harmonic mean and thus, the final 50-m resolution map for the study area was reconstructed through the linear triangulation method (Fig. 2B). Subsequently, all the hydraulic parameters were estimated for each soil and UNSZ layers down to the GWT. Also to this regard, the eventualoccurrence of areas with local heterogeneous settings were disregarded due to the regional scale of analysis and availability of data.

2.3.3. Water table depth

Piezometric levels were obtained from the GWTD map reconstructed for the study area, as described in Section 2.2.

2.3.4. Land use

To evaluate the actual evapotranspiration (ETR), both the cultivated crop and standard crop management of the area, such as seeding and harvesting dates, need to be known. In the case of the Marchfeld region, the main crops are represented by wheat, potatoes, sunflower, soya, rape, sugarbeet and maize. Accordingly, wheat was chosen as the reference crop in this study, whose management was obtained by surveys carried out among local farmers.

2.3.5. Input concentration of the solute

The TFM-ext model outputs are expressed in terms of mean TT and are independent of the solute input concentrations, given the formulation proposed by Bancheri et al. (2021). Moreover, in this study, a conservative approach was adopted considering a non-reactive solute with the assumption that it moves into the soil as water moves.

2.4. The FLOWS model

For a small sector of the Marchfeld region, identified considering results from SINTACS and TFM-ext methods, further numerical analyses were carried out to assess groundwater vulnerability at a site-specific scale, in terms of the Travel Times of a solute peak (TTp) down to the GWT. For such a scope, the FLOWS model (Coppola et al., 2019) was applied to simulate, the movement of water and solute transport through the vadose zone by a RE-ADE approach. In detail, the vertical transient water flow is simulated by numerically solving the 1D form of the RE using an implicit, backward, finite differences scheme with explicit linearization (Eq. (4)):

$$C(h)\frac{\partial h}{\partial t} = \frac{\partial}{\partial z}\left(k(h)\frac{\partial h}{\partial z} - k(h)\right) - S_w(h) \tag{4}$$

where C(h) = dθ/dh is the soil water capacity, θ [−] is the volumetric water content, h [L] is the soil water pressure head, t [T] is time, z [L] is the vertical coordinate being positive upward, and K(h) [LT^{-1}] the hydraulic conductivity, assumed to be described by the unimodal van Genuchten–Mualem model. A macroscopic sink term, $S_w(h)$ [T^{-1}], is introduced for root water uptake. According to the approach of Feddes et al. (1978), and neglecting the osmotic stress, it is calculated by the Eq. (5):

$$Sw(h) = a(h)S_p \tag{5}$$

where α(h) is the crop-specific water reduction function depending on the local (at a given z) water pressure head and S_p is the potential root uptake.

The ADE is used to predict the solute transport, both in liquid and gaseous phases, by an explicit, central difference scheme (Eq. (6)):

$$\frac{\partial \theta C}{\partial t} + \rho_b \frac{\partial C_s}{\partial t} + \frac{\partial q_g C_g}{\partial t} = -\frac{\partial qC}{\partial z} + \frac{\partial}{\partial z}\left(\theta D_h \frac{\partial C}{\partial z}\right) + \frac{\partial}{\partial z}\left(q_g D_g^s K_H \frac{\partial C}{\partial z}\right) - S_s \tag{6}$$

where, C [M L^{-3}] and C_s [M M^{-1}] are the amount of solute in the liquid and adsorbed phases, respectively, q [L T^{-1}] is the Darcian flux, ρ_b [M L^{-3}] is the bulk density, D_h [L^2 T^{-1}] the hydrodynamic dispersion coefficient, D_g^S is the dispersion coefficient in the gaseous phases [L^2 T^{-1}], θ_g is the volumetric air content in soil, K_H is the dimensionless Henry constant. S_s [$ML^{-3}T^{-1}$] is a source-sink term for solutes. The equation includes non-linear adsorption, linear decay and proportional root uptake in unsaturated/saturated soil. In this study, the applied solute was a tracer and, therefore, adsorption and decay processes were not simulated.

2.4.1. Boundary conditions for water flow and solute transport

Daily potential evapotranspiration using the Penman-Monteith equation and precipitation, referred to the period January 2013 - December 2016, were implemented as top boundary conditions. Finally, a constant potential value equal to zero was assumed as the bottom boundary condition of the model, corresponding to the water table depth determined for each soil profile. In this case, the model simulates the occurrence of a constant water table at the bottom boundary of the simulation domain.

The code allows for either constant or variable concentrations at the soil surface. The concentration used as input (C_{input}) was

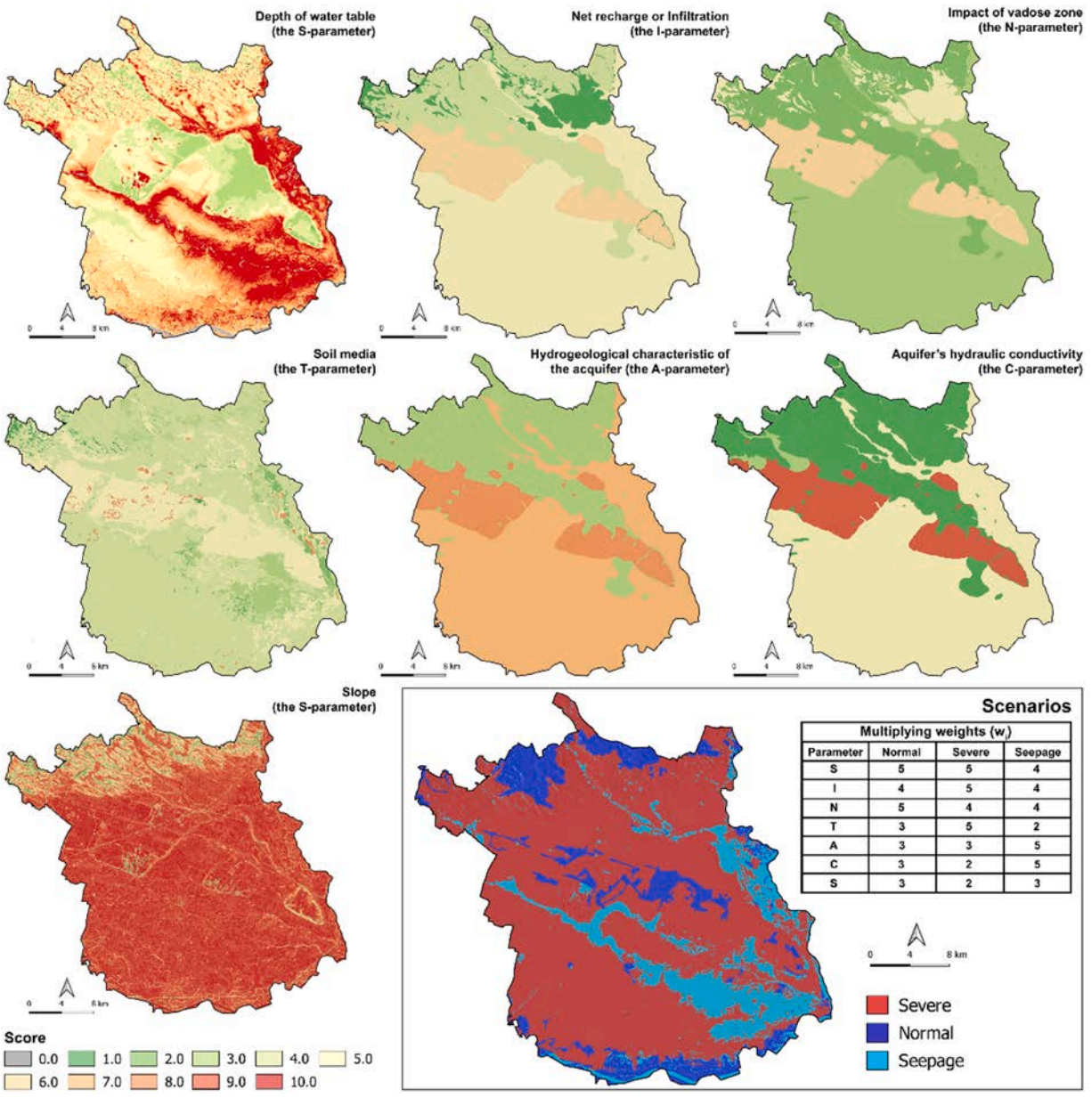

Fig. 3. - Maps of scores assigned to each parameter of the SINTACS method and the maps of scenarios from which the assignment of multiplying weights depends on.

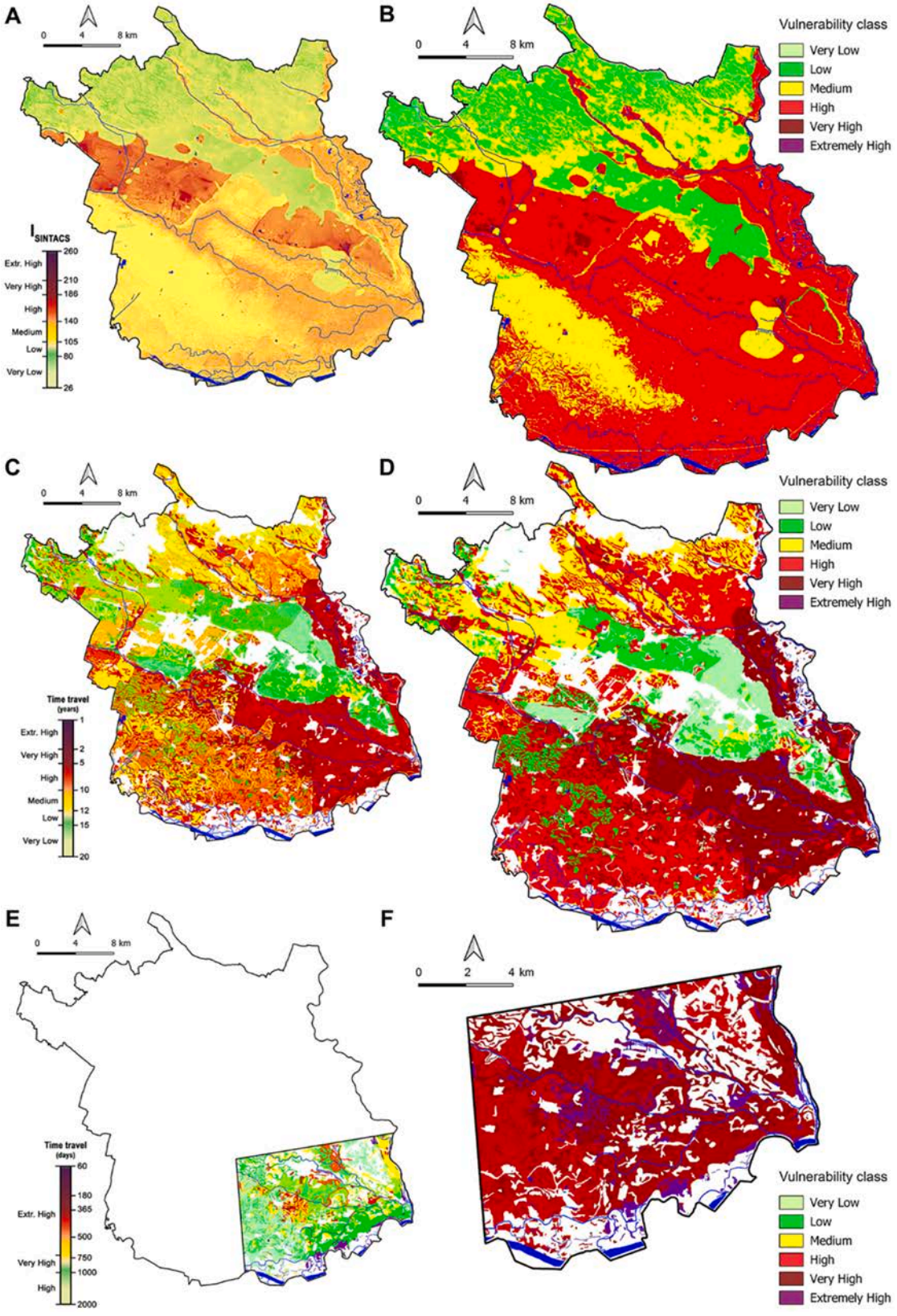

(caption on next page)

Fig. 4. - Groundwater vulnerability maps of the shallow aquifers characterizing the Marchfeld Region obtained by the application of SINTACS method (A, B), TFM-ext (C, D) and FLOWS (E, F) models.

calculated by (Eq. (7)):

$$C_{input} = \frac{Ms}{q_{surf}} \quad Dt_{app} \tag{7}$$

where q_{surf} is the top boundary flux (cm day^{-1}); Ms is the specific mass of solute applied per unit of surface area and per unit of time; Dt_{app} is the duration of the solute application.

In this study, a single pulse input of a non-reactive solute was applied for the whole simulation period on the day when there was the first precipitation event. In this way, the concentration of the solute was equal to 1.37×10^{-5} g cm^{-3}. We calculated the number of days in which the peak of the non-reactive solute was reached as the proxy for the groundwater table vulnerability.

2.4.2. Vegetation parameters

The vegetation effect was modeled considering the wheat crop parameters, as it is one of the main cultivated crops of Marchfeld. The code requires the extinction factor for the Leaf Area Index (LAI) as the exponent of Beer's law (Ritchie, 1972) for separating potential evaporation and transpiration from potential evapotranspiration. The Feddes (1978) water reduction function for root water uptake was considered as well as a uniform root distribution. Therefore, values of critical pressure heads for the latter function were set according to those typical of the wheat from the literature (Taylor et al., 1972).

2.5. Comparison of groundwater vulnerability maps

A comparison of groundwater vulnerability maps resulting from the application of each method was carried out. To homogenize $I_{SINTACS}$ and TTs values of parametric and numerical methods, respectively, the *Index of Normalization* (I_N) was defined. Such an index derives from a linear normalization of raw values (V_i), by using the following formula:

$$I_N = \frac{V_i - V_{min}}{V_{max} - V_{min}} \bullet 100$$

where V_{min} and V_{max} are the minimum and maximum $I_{SINTACS}$ and TTs raw values.

Thus, the resulting normalized values were grouped in five ranges, divided in intervals of 20 %. For the TFM-ext and FLOW methods, the resulting normalized values were inverted to be comparable with the SINTACS ones, because TT values are inversely related to the groundwater vulnerability. Subsequently, also the Pearson correlation was applied to assess how normalized values of groundwater vulnerability obtained by each method are mutually correlated. Furthermore, TT values were subdivided into six classes expressing from very low to extremely high groundwater vulnerability, according to the SINTACS classes.

Finally, to compare the spatial distribution of groundwater vulnerability values obtained by each method, a further analysis was carried out by defining the *Index of Comparison* (I_C), corresponding to the ratio of groundwater vulnerability maps according to the following pairwise ratios: SINTACS/TFM-ext, TFM-ext/FLOWS and FLOWS/SINTACS.

3. Results

3.1. Groundwater vulnerability at the regional scale

The application of the SINTACS parametric model allowed the estimation, at the regional scale, of groundwater vulnerability of the shallowest alluvial aquifers that characterize the Marchfeld region. In detail, following this approach, firstly the scores were assigned to each parameter, thus obtaining 50 m resolution raster maps (Fig. 3). Consequently, the weights were assigned considering the scenarios, as described in the 2.2 section. Generally, an intense impact characterizes most of the Marchfeld region, while the normal impact is very limited. Instead, drainage areas coincide with main rivers and their closest flooding areas, including those with values of GWTD less than 2.0 m. Once scores and weights were defined for each parameter, the map of the SINTACS index ($I_{SINTACS}$) was obtained allowing the estimation of the intrinsic groundwater vulnerability of the entire Marchfeld area. Values of $I_{SINTACS}$ range globally between 63 and 217 (Fig. 4 A) and are distributed across all six groundwater vulnerability classes, from the very low to the extremely high (Fig. 4B). In detail, values ranging between 130 and 165 characterize the RAC, thus with groundwater vulnerability crossing from medium to high classes. Higher $I_{SINTACS}$ values, ranging between 142 and 217, resulted in the AAC, coinciding with the *Gaenserndorf Terrace* especially in the area characterized by the occurrence of quarries.

The only exception is represented by the bordering slopes of the *Schlosshof Terrace*, where values range between 72 and 95, thus coinciding with lower groundwater vulnerability classes. Finally, northern areas of the Marchfeld region belonging to loess-covered Miocene hydrogeological units (LC and BAC) resulted in values of $I_{SINTACS}$ varying from 63 to 135, thus classifiable from the very low to medium groundwater vulnerability classes, with the only exception of fluvial areas (RAC) resulting comprised in the highest vulnerability one.

From TFM-ext modeling, as detailed in Section 2.3, mean values of TT of the generic non-reactive pollutant, which ranged from one

to 20 years, were obtained thus assessing groundwater vulnerability of Marchfeld at the regional scale (Fig. 4 C). For the study area, six classes, from the very low to the extremely high (Fig. 4D), were defined to compare SINTACS and TFM-ext results. Analysing the map, lower TT values were observed in the alluvial plains of the Morava and Danube rivers, where *chernozem* and *stagnic phaeozem* soils occur. Specifically, in the south-eastern part of the Marchfeld region, including part of the *Obersiebenbrunn basin*, TT values ranged between one and five years, while they increased up to 10 years moving toward the central-western part of the Danube alluvial plain. Due to both low GWTD values and the occurrence of alluvial deposits (mainly mixtures of sand and gravel), these areas were characterized by relatively faster solute TTs through the UNSZ down to the GWT.

Consequently, this part of the territory is characterized by groundwater vulnerability from high to extremely high. Instead, both in the northern and western parts of Marchfeld, covered mainly by *chernozem*, *colluvium* and *anthrosol* soils, mean TT values ranged between 11 and 13 years, although locally lower (down to 8 years) and higher (up to 15 years) values were observed. Therefore, the area can be generally classified with a medium groundwater vulnerability, with some local spots within the high and low classes. Finally, higher TT values ranging between 13 and 20 years were observed mainly in the central part of the Marchfeld region, specifically with the *Gaenserndorf Terrace* where mainly *para-chernozem* soils exist. This area is characterized by high GWTD values (6.0–15.0 m) and fine-graded deposits (loess), thus resulting in medium to very low groundwater vulnerability.

3.2. Groundwater vulnerability at the site-specific scale

A representative sub-area of the Marchfeld region, identified as highly vulnerable to pollution both by the SINTACS and TFM-ext methods, was considered for site-specific scale numerical modeling. Such a physics-based approach was intended to be the benchmark for our evaluation. The application of the FLOWS model allowed the estimation of TTs of solute peak (TTp) considering the same, non-adsorbed, non-reactive pollutant. The obtained TTp values ranged between 68 and 1484 days (Fig. 4E), thus resulting to be distributed in three groundwater vulnerability classes, from high to extremely high (Fig. 4 F), which are the same as the TFM-ext model. In detail, TTp values from 365 up to 1484 days resulted for areas with *stagnic phaeozem* soils. Values of TTp ranging between 180 and 500 days were observed both in the central and eastern sectors of the modeled area, where fluvial channels and ponds occur. Finally, the lowest TTp values (from 180 down to 68 days) characterize very localized areas where *chernozem* and *fluvisol* soils mainly exist. Consequently, the groundwater vulnerability to pollution in these latter areas resulted from very high to extremely high.

3.3. Comparison of groundwater vulnerability maps

The comparison of groundwater vulnerability maps obtained from parametric and numerical methods revealed similarities as well as relevant differences. Raw $I_{SINTACS}$ and TT values were normalized (I_N) and I_C values were defined to obtain different interpretations.

Fig. 5shows the cumulative frequency of normalized values, for the defined I_N range, and the total areas falling in each groundwater vulnerability class. In detail, the frequency distributions of normalized values from each considered method revealed comparable trends. The ~75 % of I_N values from SINTACS method are distributed covering ranges from 20 % to 80 %, while all ranges for those from TFM-ext and FLOWS ones (Fig. 5 A). Similarly, comparable results were obtained analysing the frequency distributions of areas falling in each vulnerability class. In fact, the TFM-ext method classifies the study area as characterized by all vulnerability classes, while from low to very high and from very high to extremely high for SINTACS and FLOWS, respectively (Fig. 5B). Such a condition revealed by FLOWS results is strongly related to the different extension of the considered site-specific scale area.

Fig. 6 shows maps of the spatial distribution of I_C values obtained considering the assessed raw groundwater vulnerability values (Fig. 6A-B-C) and classes (Fig. 6D-E-F). Such index was conceived as the ratio of SINTACS/TFM-ext, TFM-ext/FLOWS and FLOWS/SINTACS groundwater vulnerability maps, respectively. Resulting I_C maps were analysed, and the cumulative frequency of both groundwater vulnerability values and class for I_C ranges are reported in Fig. 7.

The frequency distributions of I_C values revealed a strong correlation between TFM-ext and FLOWS methods while slightly lower between SINTACS and numerical ones. At the regional scale, the comparison of SINTACS and TFM-ext maps revealed that ~58 % of I_C values range between 0.75 and 1.25. The remaining ones resulted to be characterized by I_C values <0.75 and >1.25 (~37 % of total), thus resulting in different vulnerability degrees. At the site-specific scale, the comparison of FLOWS results with those of TFM-ext and SINTACS methods also revealed a good matching between approaches. In fact, ~93 % of the site-specific area resulted for both FLOW and TFM-ext models as the most vulnerable, from high to extremely high, with values of I_C ranging between 0.75 and 1.25, while ~77 % of the areas resulted coinciding for SINTACS and FLOWS.

The best correlation was found between TFM-ext and FLOWS (corr. = 0.53) with the highest statistical significance, followed by SINTACS-TFM-ext (corr. = 0.25). In contrast, the correlation between SINTACS and FLOWS (corr. = 0.05) was found to be the poorest one, due to the different parameters involved in the vulnerability assessment.

4. Discussion

Results obtained in this study represent advances in the assessment of groundwater vulnerability in complex and intensively cultivated alluvial hydrogeological frameworks, such as the Marchfeld region, where industrial and agricultural activities are the main causes of the decay of groundwater quality. Given the different spatial density and quality of data needed by parametric and numerical methods for estimating groundwater vulnerability and consequently the greater difficulty to apply the second ones, a comparison among results of both types of methods is conceived as useful to understand mutual potentialities and limitations. This is motivated by the level of complexity of numerical methods, depending on data required to solve equations for flow and transport processes in

unsaturated and/or saturated porous media, which strongly affects their applicability.

Aiming at selecting the most appropriate method for estimating groundwater vulnerability, several studies were based on the comparison of the performance of different methods in different hydrogeological and environmental conditions. Generally, the comparative assessment was performed using DRASTIC-like methods, as in the case of a detrital aquifer in Morocco (Draoui et al., 2008) or of porous ones in Greece (Kirlas et al., 2022). Instead, the comparison of parametric and numerical methods, such as the case of Charmahal-Bakhtyari Province in Iran (Abbasi et al., 2013), appears rare and rather conceived as a challenge for researchers. In fact, this type of comparison is not advisable because qualitative and quantitative approaches are very differently structured, so results might be incomparable.

Therefore, the assessment of groundwater vulnerability for Marchfeld region, proposed in this study by the comparison of parametric and numerical methods, applied from regional to site-specific scales respectively, revealed how results of a DRASTIC-like method, such as SINTACS, and two numerical process-based ones, such as TFM-ext and FLOWS, can deliver hints regarding the respective potentialities and limitations. The approach follows the trend of recent studies focused on emphasizing the reliability of parametric methods and by the comparison of their results with those obtained by the numerical ones (Machiwal et al., 2018).

Results obtained by the SINTACS parametric method, at the regional scale, by the TFM-ext and agro-hydrological FLOWS numerical models, and the site-specific scale, showed the large variability of groundwater vulnerability due to hydrological, morphological and anthropic conditions. The distribution of both $I_{SINTACS}$ and TT values revealed how the RAC, characterized by high-permeability deposits (ranging from sands to gravels and cobbles) and lower GWTD values, resulted generally being the most vulnerable with both types of models. Moreover, by the application of FLOWS, at site-specific scale, a greater area with “extremely high” groundwater vulnerability was identified. Concerning the LC, BAC and RFAC, a groundwater vulnerability grade from “low” to “medium” was recognized. The low permeability characterizing such deposits, varying from clays to sands, leads to a reduction of the velocity of the infiltration processes thus favouring a major attenuation of potential pollutant effects. Finally, the AAC resulted to be characterized by higher vulnerability classes, from “high” to “extremely high”, through the application of SINTACS, while from “very low” to “high” ones through the TFM-ext model. The combined application of parametric and numerical models appears particularly suitable for

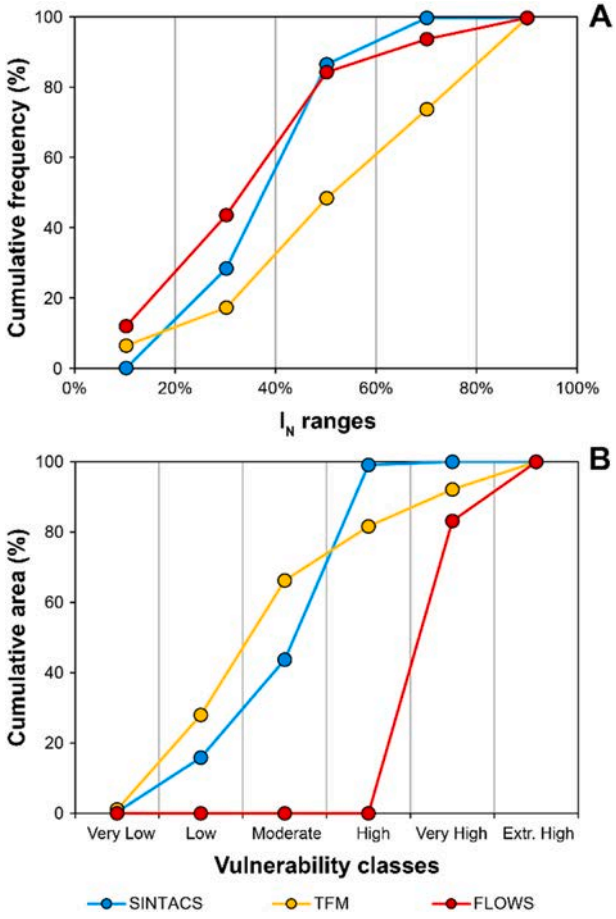

Fig. 5. - Frequency distribution of normalized index values (A) and areas for each vulnerability class (B), resulted by SINTACS, TFM-ext and FLOWS methods application. I_N are grouped in five 20 %-ranges, while areas are reported as percentage related to regional scale area, for SINTACS and TFM-ext methods, and site-specific one, for FLOWS method.

multi-scale analysis, such as the one presented in this work, according to other studies (Machiwal et al., 2018; Cusano et al., 2019).

In general, the assessment of groundwater vulnerability classes by different methods showed a consistent matching although differences for some specific areas. To perform a quantitative comparison, raw values of groundwater vulnerability obtained by SINTACS, TFM-ext and FLOWS methods were converted into normalized indexes (I_N). Moreover, a comparison ratio (I_C) was calculated and mapped by rating the assessed groundwater vulnerability values and classes. At the regional scale, SINTACS and TFM-ext

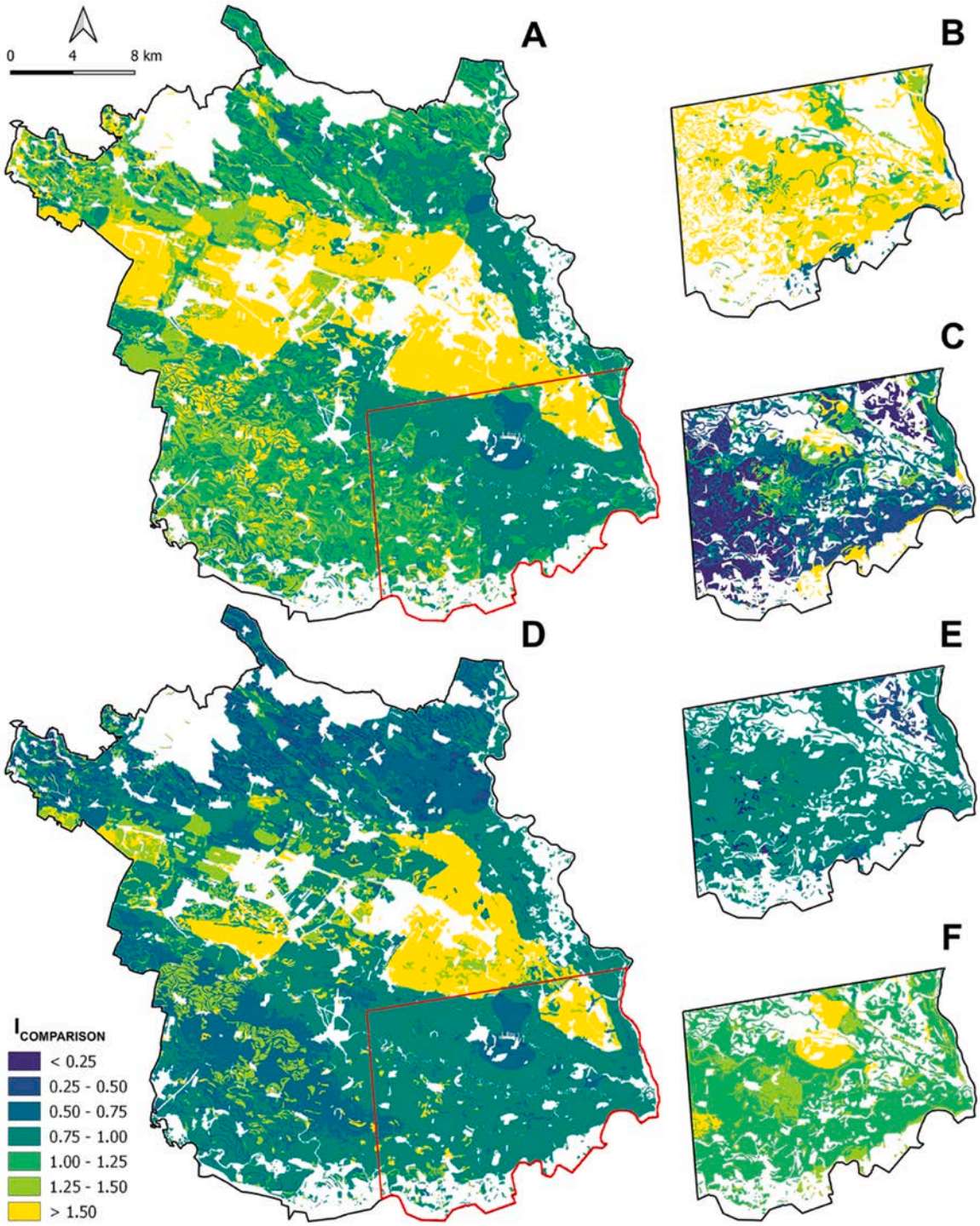

Fig. 6. - Index of Comparison (I_C) obtained by rating maps of raw groundwater vulnerability values (A-B-C) and classes (D-E-F) as following: SINTACS/TFM-ext (A), TFM-ext/FLOWS (B) and FLOWS/SINTACS (C).

maps revealed that alluvial aquifers resulted with comparable groundwater vulnerability classes. Only those locally coinciding with hilly northern and central sectors of the region, resulted in different groundwater vulnerability degrees. According to other researchers (Neukum and Azzam, 2009; Kazakis and Voudouris, 2015; Cusano et al., 2019; Fusco at el., 2020; Nasta et al., 2021; Cusano et al., 2023), types of lithology and GWTDs resulted the most influencing parameters for both approaches. Specifically, results of SINTACS revealed how the type of unsaturated and saturated zone of the aquifer, the N and A parameters respectively, are the most sensitive parameters which strongly affect the results. Both parameters were set as equal, depending on the scale of analysis and the available hydrogeological information. On the contrary, with the TFM-ext model, the GWTD resulted in controlling the assessment of the mean TT more than the soil hydrological properties and transport parameters. Usually, they play an important role in solute transport (Coppola et al., 2009) and, in this work, they were derived using the HYPRES pedotransfer functions. The latter, as well as the other PTFs, determined a smoothing of the natural spatial variability of the hydraulic properties within the investigated region (Basile et al., 2019). Such considerations are revealed by results obtained for large areas of the Marchfeld region coinciding with the AAC, such as those of the *Gaeserndorf* and the *Schlosshof* terraces, and with both the LC and BAC, mainly including the northern sector. The first ones, characterized by high GWTD values and coarser aquifer lithologies, resulted with a higher groundwater vulnerability by the parametric method more than the numerical one. Instead, the second one, characterized by low-permeable lithologies and low GWTD values, resulted with higher values of groundwater vulnerability by the application of the TFM-ext model more than the SINTACS one. At the site-specific scale, the comparison of FLOWS results with those of TFM-ext and SINTACS methods also revealed a general positive correlation between approaches. The best correlation was obtained between FLOWS and TFM-ext models, with almost the total area resulting as the most vulnerable, while the poorest between SINTACS and FLOWS ones. Such an outcome can be related to the type of analysis performed by FLOWS model, in which soil types and properties and GWTDs resulted in the most influencing parameters. Being FLOWS a physics-based model reliant on Richards' model (Richards, 1931), it allows performing transient state modeling of solute infiltration, solving the water balance and simulating all the water fluxes, such as the water uptake and groundwater recharge, besides the solute breakthrough curves. From this point of view, the model can be considered as the reference for the assessment of the evaluation of the goodness of agreement between the identified vulnerability classes. Poor correlation between the results of SINTACS and FLOWS methods emphasizes the relevant effect of time-variable parameters, such as rainfall intensity and evapotranspiration, and other physical and chemical processes controlling the fate and transport of contaminants in the UNSZ.

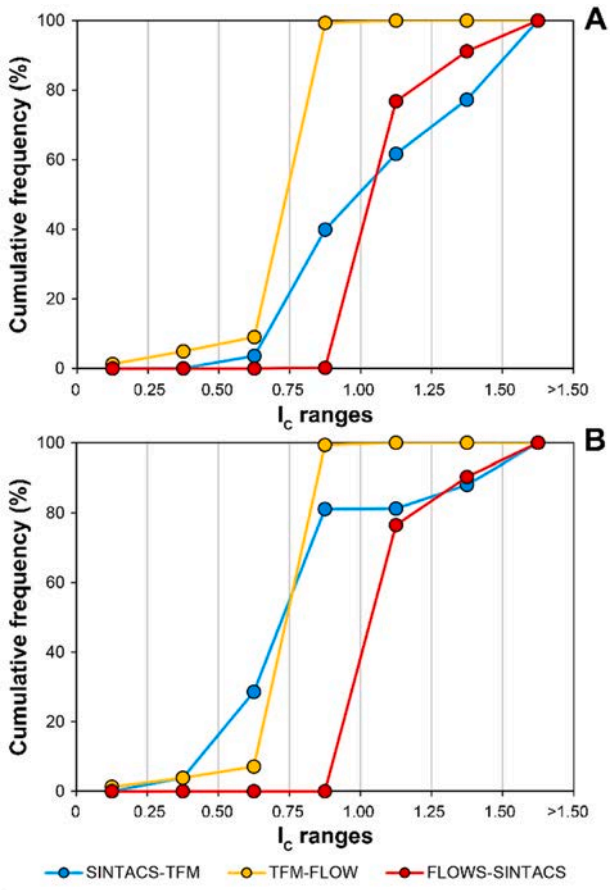

Fig. 7. - Frequency distribution of the Index of Comparison (I_C) values referred to normalized index values maps (A) and vulnerability class (B), obtained by rating maps of groundwater vulnerability as following: SINTACS/TFM-ext (A), TFM-ext/FLOWS (B) and FLOWS/SINTACS (C).

Results from this study agree with other ones where physics-based travel time and quantitative rating methods were coupled to assess aquifer vulnerability in Huangshuihe catchment, China (Yu et al., 2010), and in Neon Sidirochorion aquifer, Northeastern Greece (Pisinaras et al., 2016). Therefore, pairwise comparisons of SINTACS-FLOWS and TFM-FLOWS led to consider SINTACS and TFM-ext methods as very comparable and suitable for regional-scale analysis, while FLOWS is suitable for further analysis at a site-specific scale. However, some specific assumptions of the adopted approaches could represent potential limitations. Specifically, it should be mentioned that the areas with local complex heterogeneous hydrogeological settings, such as those with high-density paleochannels (Figs. 1B and 2B). This simplification is related to the type and spatial distribution of input 1D stratigraphic and hydrogeological data as well as by the regional scale of the adopted methods. Moreover, depending on data availability and the scale of analysis, no 3D hydrogeological models were reconstructed. Furthermore, the estimation of the net recharge and the hydraulic conductivity parameters was based on empirical and quali-quantitative approaches, depending on the availability of hydrological and hydrogeological data. Therefore, all possible limitations affecting the adopted approach were considered acceptable due to the regional scale of analysis and being aware that the assessment of groundwater vulnerability at the local scale would require spatially-dense and high-quality input data (Cusano et al., 2019).

However, deriving from the above discussions, the approach presented in this study to assess groundwater vulnerability for the Marchfeld region can be conceived as advancing those obtained by the use of field data and tools of Geographic Information System (GIS) platforms (Corniello et al., 2007; Liggett and Allen, 2011; Tufano et al., 2020) or in other cases coupled with the estimated TT of pollutants through the vadose zone (Connell et al., 2003; Voigt et al., 2004; Yu et al., 2010; Wang et al., 2012; Fetisova et al., 2016; Nolan et al., 2018; Cusano et al., 2019; Fusco et al., 2020).

5. Conclusions

The goal of this study was the comparative estimation and mapping of groundwater vulnerability of shallow alluvial aquifers by a multi-method approach applied at different spatial scales, from regional to site-specific one. The approach proposed is based on the combination of parametric methods, to assess the intrinsic vulnerability of shallow aquifers, and numerical ones, to perform numerical modeling of pollutant mean travel time through the unsaturated zone. To such a scope, the Marchfeld region was considered as representative of similar others affected by hydro-chemical decay of groundwater quality due to intensive agriculture. Thus, assessing groundwater vulnerability is crucial for proper land planning and management, as well as the implementation of effective groundwater protection strategies.

An important effort was the comparison of results which revealed very coherent outcomes, despite differences between parametric and numerical models. Specifically, such a comparison emphasized how the assessment of groundwater vulnerability, based on applying the parametric SINTACS method and the numerical TFM-ext and FLOWS ones, was strongly affected by the type and spatial-temporal features of the available data.

The proposed comparative approach between different methods used for the assessment of groundwater vulnerability resulted in very useful in revealing similarities and limitations to be used for selecting the most appropriate one.

The presented study advances the knowledge about the assessment of groundwater vulnerability in areas affected by intensive agricultural activities. Specifically, results are expected to be considered by a wide range of stakeholders such as land managers (i.e., public authorities), to properly evaluate more informed decisions regarding which areas the pollution from agricultural activities should be primarily reduced.

Funding

This research was funded by the EC H2020 LANDSUPPORT project (grant number: 774234. P.I. Fabio Terribile) and project PNRR GEOSCIENCES IR, Mission 4, CUP 153C22000800006.

CRediT authorship contribution statement

Antonio Coppola: Writing – review & editing, Validation, Software, Methodology, Investigation, Data curation. **Martin Neuwirth:** Data curation. **Angelo Basile:** Writing – review & editing, Validation, Supervision, Software, Methodology, Investigation, Data curation. **Domenico Calcaterra:** Writing – review & editing, Supervision. **Pantaleone De Vita:** Writing – review & editing, Validation, Supervision, Methodology, Conceptualization. **Angela Puig-Sirera:** Validation, Software, Methodology, Investigation, Data curation. **Fabio Terribile:** Writing – review & editing, Project administration, Funding acquisition. **Marialaura Bancheri:** Writing – review & editing, Writing – original draft, Visualization, Validation, Software, Resources, Methodology, Investigation, Formal analysis, Data curation. **Francesco Fusco:** Writing – review & editing, Writing – original draft, Visualization, Validation, Resources, Methodology, Formal analysis, Data curation, Conceptualization. **Vincenzo Allocca:** Writing – review & editing, Validation, Methodology, Conceptualization.

Declaration of Competing Interest

The authors declare that they have no known competing financial interests or personal relationships that could have appeared to influence the work reported in this paper.

Data Availability

Data will be made available on request.

Acknowledgments

Authors sincerely thank the Editor and the anonymous for having provided valuable suggestions aimed at the improvement of both the quality and consistency of the manuscript.

Appendix A. Supporting information

Supplementary data associated with this article can be found in the online version at doi:10.1016/j.ejrh.2024.101865.

References

Abbasi, S., Mohammadi, K., Kholghi, M.K., Howard, K., 2013. Aquifer vulnerability assessments using DRASTIC, Weights of Evidence and the Analytic Element Method. Hydrol. Sci. J. 58 (1), 1–12. https://doi.org/10.1080/02626667.2012.743027.

AGI, 1977. AGI (1977) – Raccomandazioni su programmazione ed esecuzione delle indagini geotecniche..

Albinet, M., Margat, J., 1970. Cartographie de la vulnérabilité à la pollution des nappes d'eau souterraine. Bull. BRGM 2, 4.

Allen, R.G., Pereira, L.S., Raes, D., Smith, M., et al., 1998. Crop evapotranspiration-Guidelines for computing crop water requirements- FAO Irrigation and drainage paper 56. Fao, Rome 300, D05109.

Aller, L., Bennet, T., Lehr, J.H., Petty, R.J., Hackett, G., 1985. In: Robert, S., Kerr. (Eds.), DRASTIC: a standardized system for evaluating ground water pollution potential using hydrogeologic settings. Environmental Research Laboratory, Office of Research and Development, US Environmental Protection Agency.

Bancheri, M., Coppola, A., Basile, A., 2021. A new transfer function model for the estimation of non-point-source solute travel times. J. Hydrol., 126157 https://doi.org/10.1016/j.jhydrol.2021.126157.

Basile, A., Bonfante, A., Coppola, A., De Mascellis, R., Falanga Bolognesi, S., Terribile, F., Manna, P., 2019. How does PTF interpret soil heterogeneity? A stochastic approach applied to a case study on maize in Northern Italy. Water 11 (2), 275. https://doi.org/10.2136/vzj2005.0128.

Brouyère, S., Jeannin, P.Y., Dassargues, A., Goldscheider, N., Popescu, I.C., Sauter, M., Vadillo, I., Zwahlen, F. (2001) Evaluation and validation of vulnerability concepts using a physically based approach. In Proceedings of the 7th Conference on Limestone Hydrology and Fissured Media, Mémoire no. 13, Sciences et Techniques de l'Environnement, Université de Franche-Comté, Besançon, France, 20–22 September 2001.

Civita, M., 1994. Contamination Vulnerability Mapping of the Aquifer: Theory and Practice. Quaderni di Tecniche di Protezione Ambientale. Pitagora Editor.

Civita, M., 2010. The combined approach when assessing and mapping groundwater vulnerability to contamination. J. Water Resour. Prot. 2-1, 14–28. https://doi.org/10.4236/jwarp.2010.21003.

Civita, M., De Maio, M., 2000. SINTACS R5 a new parametric system for the assessment and automatic mapping of groundwater vulnerability to contamination. Pitagora Editor, Bologna, p. 226.

Connell, L., Van, den, Daele, G., 2003. A quantitative approach to aquifer vulnerability mapping. J. Hydrol. 276, 71–88. https://doi.org/10.1016/S0022-1694(03)00038-6.

Coppola, A., Comegna, V., Basile, A., Lamaddalena, N., Severino, G., 2009. Darcian preferential water flow and solute transport through bimodal porous systems: experiments and modelling. J. Contam. Hydrol. 104 (1-4), 74–83. https://doi.org/10.1016/j.jconhyd.2008.10.004.

Coppola, Dragonetti, G., Comegna, A., Zdruli, P., Lamaddalena, N., Pace, S., De Simone, L., 2014. Mapping solute deep percolation fluxes at regional scale by integrating a process-based vadose zone model in a Monte Carlo approach. Soil Sci. Plant Nutr. https://doi.10.1080/00380768.2013.855615N.

Coppola, A., Dragonetti, G., Sengouga, A., Lamaddalena, N., Comegna, A., Basile, A., Noviello, N., Nardella, L., 2019. Identifying optimal irrigation water needs at district scale by using a physically based agro-hydrological model. Water 11, 841. https://doi.org/10.3390/w11040841.

Corniello, A., Ducci, D., Ruggieri, G., 2007. Areal identification of groundwater nitrate contamination sources in periurban areas. J. Soils Sediment. 7, 159–166. https://doi.org/10.1065/jss2007.03.213.

Cusano, D., Allocca, V., Fusco, F., Tufano, R., De Vita, P., 2019. Multi-scale assessment of groundwater vulnerability to pollution: study cases from Campania region (Southern Italy). Ital. J. Eng. Geol. Environ. 19–24. https://doi.org/10.4408/IJEGE.2019-01.S-03.

Cusano, D., Coda, S., De Vita, P., Fabbrocino, S., Francesco, F., Lepore, D., Nicodemo, F., Pizzolante, A., Tufano, R., Allocca, V., 2023. A comparison of methods for assessing groundwater vulnerability in karst aquifers: the case study of Terminio Mt. aquifer (Southern Italy). Sustain Environ. Res 33, 42. https://doi.org/10.1186/s42834-023-00204-8.

Darsow, A., Schafmeister, M.T., Hofmann, T., 2009. An ArcGIS-approach to include tectonic structures in point data regionalization. Groundwater 47 (4), 591–597. https://doi.org/10.1111/j.1745-6584.2009.00546.x.

De Vita, P., Allocca, V., Celico, F., Fabbrocino, S., Mattia, C., Monacelli, G., Musilli, I., Piscopo, V., Scalise, R.A., Summa, G., et al., 2018. Hydrogeology of continental southern Italy. J. Maps 14, 230–241. https://doi.org/10.1080/17445647.2018.1454352.

Decker, K., Peresson, H., Hinsch, R., 2005. Active tectonics and Quaternary basin formation along the Vienna Basin Transform fault. ISSN 0277-3791 Quat. Sci. Rev. Volume 24 (Issues 3–4), 305–320. https://doi.org/10.1016/j.quascirev.2004.04.012.

Doppler, G., Kroemer, E., Rögner, K., Wallner, J., Jerz, H., Grottenthaler, W., 2011. Quaternary stratigraphy of southern Bavaria. / number 2–3 / 2011 / Quat. Sci. J. Volume 60, 329–365. https://doi.org/10.3285/eg.60.2-3.08.

Draoui, M., Vias, J., Andreo, B., Targuisti, K., El Messari, J.S., 2008. A comparative study of four vulnerability mapping methods in a detritic aquifer under mediterranean climatic conditions. Environ. Geol. 54, 455–463. https://doi.org/10.1007/s00254-007-0850-3.

Fank, J., Rock, G., Dalla Via, A., Poltnig, W., Draxler, J.C., Plieschnegger, M., 2008. Grundwasserströmungsmodell Marchfeld. Institut für Wasser Ressourcen. Management Hydrogeologie und Geophysik. April, 2008.

Feddes, R., Kowalik, P., Zaradny, H. Simulation of field water use and crop yield. Simul. Monog. PUDOC, Wageningen, the Netherlands. Simulation of field water use and crop yields. Simul. Monogr. Pudoc, Wageningen, the Netherlands. 1978.

Fetisova, N.F., Fetisov, F.F., De Maio, M., Zektser, I.S., 2016. Groundwater vulnerability assessment based on calculation of chloride travel time through the unsaturated zone on the area of the Upper Kama potassium salt deposit. Environ. Earth Sci. 75, 681. https://doi.org/10.1007/s12665-016-5496-6.

Foster, S., 1987. Foster, S. Fundamental concepts in aquifer vulnerability, pollution risk and protection strategy 1987..

Freeze, R., Cherry, J. Groundwater, Prentice-hall, 1979.

Fusco, F., Allocca, V., Coda, S., Cusano, D., Tufano, R., De Vita, P., 2020. Quantitative assessment of specific vulnerability to nitrate pollution of shallow alluvial aquifers by process-based and empirical approaches. Water 12, 269. https://doi.org/10.3390/w12010269.

Geiger, R.Landolt-B.örnstein – Zahlenwerte und Funktionen aus Physik, Chemie, Astronomie, Geophysik und Technik, alte Serie Vol. 3, in: Klassifikation der Klimate nach W. Köppen, Springer, Berlin, 1954, 603–607.

Gogu, R.C., Dassargues, A., 2000. Current trends and future challenges in groundwater vulnerability assessment using overlay and index methods. Environ. Geol. 39, 549–559. https://doi.org/10.1007/s002540050466.
Healy, R.W. Estimating groundwater recharge, Cambridge university press, 2010; https://doi.org/10.1017/CBO9780511780745.
Hölzel, M., Wagreich, M., Faber, R., Strauss, P., 2008. Regional subsidence analysis in the Vienna Basin (Austria). Austrian J. Earth Sci. Volume 101, 88–98. Vienna 2008.
Jury, W.A., Roth, K., et al. Transfer functions and solute movement through soil: Theory and applications., Birkhäuser Verlag AG, 1990.
Kazakis, N., Voudouris, K.S., 2015. Groundwater vulnerability and pollution risk assessment of porous aquifers to nitrate: Modifying the DRASTIC method using quantitative parameters. J. Hydrol. 525, 13–25. https://doi.org/10.1016/j.jhydrol.2015.03.035.
Kirchner, M., Schmid, E., 2012. Kirchner, M., Schmid, E. How Do Agricultural Trade Policies Affect The Regional Environment? An Integrated Analysis For The Austrian Marchfeld Region. Technical report, 2012; https://doi.org/10.22004/ag.econ.137160..
Kirlas, M.C., Karpouzos, D.K, Georgiou, P.E., et al., 2022. A comparative study of groundwater vulnerability methods in a porous aquifer in Greece. Appl. Water Sci. 12, 123. https://doi.org/10.1007/s13201-022-01651-1.
Liggett, J.E., Allen, D.M., 2011. Evaluating the sensitivity of DRASTIC using different data sources, interpretations and mapping approaches. Environ. Earth Sci. 62, 1577–1595. https://doi.org/10.1007/s12665-010-0642-z.
Lindblom, J., Ljung, M., Jonsson, A., 2017. Promoting sustainable intensification in precision agriculture: review of decision support systems development and strategies. Precis. Agric. 18, 309–331. https://doi.org/10.1007/s11119-016-9491-4.
Machiwal, D., Jha, M.K., Singh, V.P., Mohan, C., 2018. Assessment and mapping of groundwater vulnerability to pollution: current status and challenges. Earth Sci. Rev. 185, 901–927. https://doi.org/10.1016/j.earscirev.2018.08.009.
Manna, P., Bonfante, A., Colandrea, M., Di Vaio, C., Langella, G., Marotta, L., Mileti, F.A., Minieri, L., Terribile, F., Vingiani, S., et al., 2020. A geospatial decision support system to assist olive growing at the landscape scale. Comput. Electron. Agric. 168, 105143 https://doi.org/10.1016/j.compag.2019.105143.
Marano, G., Langella, G., Basile, A., Cona, F., De Michele, C., Manna, P., Teobaldelli, M., Saracino, A., Terribile, F., 2019. A geospatial decision support system tool for supporting integrated forest knowledge at the landscape scale. Forests 10, 690. https://doi.org/10.3390/f10080690.
Nasta, P., Bonanomi, G., Šimůnek, J., Romano, N., 2021. Assessing the nitrate vulnerability of shallow aquifers under Mediterranean climate conditions. ISSN 0378-3774 Agric. Water Manag. 258, 107208. https://doi.org/10.1016/j.agwat.2021.107208.
National Research Council (NRC, 1993. Nutrient requirements of fish. National Academy Press, Washington DC.
Neukum, C., Azzam, R., 2009. Quantitative assessment of intrinsic groundwater vulnerability to contamination using numerical simulations. Sci. Total Environ. 408, 245–254. https://doi.org/10.1016/j.scitotenv.2009.09.046.
Nicholson, F., Krogshave Laursen, R., Cassidy, R., Farrow, L., Tendler, L., Williams, J., Surdyk, N., Velthof, G., 2020. How can decision support tools help reduce nitrate and pesticide pollution from agriculture? A literature review and practical insights from the EU fairway project. Water 12, 768. https://doi.org/10.3390/w12030768.
Nolan, B.T., Green, C.T., Juckem, P.F., Liao, L., Reddy, J.E., 2018. Metamodeling and mapping of nitrate flux in the unsaturated zone and groundwater, Wisconsin, USA. J. Hydrol. 559, 428–441. https://doi.org/10.1016/j.jhydrol.2018.02.029.
Pisinaras, V., Polychronis, C., Gemitzi, A., 2016. Intrinsic groundwater vulnerability determination at the aquifer scale: a methodology coupling travel time estimation and rating methods. Environ. Earth Sci. 75 https://doi.org/10.1007/s12665-015-4965-7.
Richards, L.A., 1931. Capillary conduction of liquids through porous medium. Physics 1, 318. https://doi.org/10.1063/1.1745010.
Ritchie, Joe T., 1972. Model for predicting evaporation from a row crop with incomplete cover. Water Resour. Res. 8 (5), 1204–1213. https://doi.org/10.1029/WR008i005p01204.
Scotter, D., Ross, P., 1994. The upper limit of solute dispersion and soil hydraulic properties. Soil Sci. Soc. Am. J. 58, 659–663.
Stewart, I.T., Loague, K., 2003. Development of type transfer functions for regional-scale nonpoint source groundwater vulnerability assessments. Water Resour. Res. 39 https://doi.org/10.1029/2003WR002269.
Sterling A., and Gaylen L. Ashcroft. Physical edaphology. The physics of irrigated and nonirrigated soils. 1972; https://doi.org/10.2134/jeq1974.00472425000300020028x.
Terribile, F., Acutis, M., Agrillo, A., Anzalone, E., Azam-Ali, S., Bancheri, M., Basile, A., 2023. The LANDSUPPORT geospatial decision support system (S-DSS) vision: operational tools to implement sustainability policies in land planning and management. Land Degrad. Dev. 35 (2), 813–834. https://doi.org/10.1002/ldr.4954.
Tufano, R., Allocca, V., Coda, S., Cusano, D., Fusco, F., Nicodemo, F., Pizzolante, A., De Vita, P., 2020. Groundwater vulnerability of principal aquifers of the Campania region (southern Italy). J. Maps 16, 565–576. https://doi.org/10.1080/17445647.2020.1787887.
Turc, L., 1954. Le bilan d'eau des sols: Relations entre les precipitations, l'evaporation et l'ecoulement. Ann. Agron. 5, 5–131, 491-595; 6.
Van Genuchten, M.T., 1980. A closed-form equation for predicting the hydraulic conductivity of unsaturated soils. Soil Sci. Soc. Am. J. 44, 892–898. https://doi.org/10.2136/sssaj1980.03615995004400050002x.
Voigt, H.-J., Heinkele, T., Jahnke, C., Wolter, R., 2004. Characterization of groundwater vulnerability to fulfill requirements of the water framework directive of the European Union. GeofiS. Int. 43, 567–574.
Wang, J., He, J., Chen, H., 2012. Assessment of groundwater contamination risk using hazard quantification, a modified DRASTIC model and groundwater value, Beijing Plain, China. Sci. Total Environ. 432, 216–226. https://doi.org/10.1016/j.scitotenv.2012.06.005.
Weissl, M., Hintersberger, E., Lomax, J., Lüthgens, C., Decker, K., 2017. Active tectonics and geomorphology of the Gaenserndorf Terrace in the Central Vienna Basin (Austria). ISSN 1040-6182 Quat. Int. 451 (2017), 209–222. https://doi.org/10.1016/j.quaint.2016.11.022.
Wessely, G., 1993. Geologischer Tiefbau Wiener Becken—Molasse Niederösterreichs. In: Brix, F., Schulz, O. (Eds.), Erdöl und Erdgas in Österreich, Wien, Beil.
Wessely, G., Draxler, I., 2006. Pliozän und Quartär. Niederösterreich. Geol. der Österreichischen Bundesl. änder 235–252.
Wösten, J., Pachepsky, Y.A., Rawls, W., 2001. Pedotransfer functions: bridging the gap between available basic soil data and missing soil hydraulic characteristics. J. Hydrol. 251, 123–150. https://doi.org/10.1016/S0022-1694(01)00464-4.
Yalew, S., Van Griensven, A., van der Zaag, P., 2016. Agrisuit: a web-based gis-mcda framework for agricultural land suitability assessment. Comput. Electron. Agric. 128, 1–8. https://doi.org/10.1016/j.compag.2016.08.008.
Yu, C., Yao, Y., Hayes, G., Zhang, B., Zheng, C., 2010. Quantitative assessment of groundwater vulnerability using index system and transport simulation, Huangshuihe catchment, China. Sci. Total Environ. 408, 6108–6116. https://doi.org/10.1016/j.scitotenv.2010.09.002.
Zaza, C., Bimonte, S., Faccilongo, N., La Sala, P., Gallo, C., 2018. A new decision-support system for the historical analysis of integrated pest management activities on olive crops based on climatic data. Comput. Electr. Agric. 148, 237–249. https://doi.org/10.1016/j.compag.2018.03.015.
Zektser, Igor S., Everett, Lorne G., 2000. Groundwater and the environment: applications for the global community. CRC Press.
Zhang, R., 2000. Generalized transfer function model for solute transport in heterogeneous soils. Soil Sci. Soc. Am. J. 64, 1595–1602. https://doi.org/10.2136/sssaj2000.6451595x.